

# Dependence of far-field characteristics on the number of lasing modes in stadium-shaped InGaAsP microlasers

Muhan Choi\*, Susumu Shinohara, and Takahisa Harayama  
 Department of Nonlinear Science, ATR Wave Engineering Laboratories,  
 2-2-2 Hikaridai, Seika-cho, Soraku-gun, Kyoto 619-0288, Japan

## Abstract

We study spectral and far-field characteristics of lasing emission from stadium-shaped semiconductor (InGaAsP) microlasers. We demonstrate that the correspondence between a lasing far-field emission pattern and the result of a ray simulation becomes better as the number of lasing modes increases. This phenomenon is reproduced in the wave calculation of the cavity modes.

## 1 Introduction

Two-dimensional (2D) optical microcavities have been attracting the attention of many researchers, on one hand because of their potential applications in optical engineering [1] and on the other hand because they offer an experimental testing ground for the quantum/wave chaos theory [2]; the basic formalism for the wave description of a quantum billiard can be applied with some little modifications to the description of the light field confined in a 2D optical microcavity [3]. One of the simplest cavity shapes that are interesting from the viewpoint of the quantum/wave chaos theory is the shape called the Bunimovich stadium, as illustrated in the inset of Fig. 1(a). This shape is well known for its mathematically proven property that a billiard ball or a ray inside the cavity exhibits fully chaotic dynamics [4].

The idea of using the stadium shape as a laser cavity has been examined both theoretically and experimentally [5, 6, 7, 8, 9, 10, 11]. Actual stadium-shaped microcavities have been fabricated using materials such as semiconductors [7, 8, 9, 10] and polymers [11]. A remarkable property that is commonly observed for relatively large cavity sizes is that the lasing emission patterns can be well explained by a ray model [7, 8, 11]. The ray model can be regarded as an open Hamiltonian system, whose openness, that is the light leakage at the cavity boundary, is described by Fresnel's law [2, 3]. A theoretical mechanism leading to the correspondence between ray and wave descriptions has been numerically investigated in Refs. [6, 7]. In the present paper, we report experimental results on the dependence of far-field emission patterns on the number of lasing modes for stadium-shaped microlasers, revealing that the good correspondence with the result of a ray simulation is obtained when multiple modes are involved in lasing.

We carried out experiments for stadium-shaped microcavities with strained InGaAsP multiple-quantum-well separate-confinement-heterostructures, the detail of whose layer structures has been reported in Ref. [12]. The radius  $R$  of the semi-circular parts of the stadium is  $15\ \mu\text{m}$ . The main difference between InGaAsP cavities and GaAs cavities used in previous works [7, 8] is that the lasing wavelength of the former,  $\lambda \approx 1558\ \text{nm}$ , is almost twice as large as that of the latter,  $\lambda \approx 850\ \text{nm}$ . That means, for fixed  $R$ , the dimensionless size parameter  $nkR = 2n\pi R/\lambda$  for an InGaAsP cavity is almost half of that for a GaAs cavity, since the effective refractive index of InGaAsP,  $n = 3.23$ , is almost same as that of GaAs,  $n = 3.3$ . For our InGaAsP cavity,  $nkR$  becomes around 195, for which we are able to perform the wave calculation of cavity modes based on the boundary element method [13] and found that the average mode spacing is large enough to resolve individual modes with the resolution of our spectrometer.

## 2 Spectral characteristics

We electrically pump the laser at room temperature using a pulsed current of 30ns-width with 1% duty cycle. In our experiment, setting the pulse width short is crucial for maintaining thermal stability

---

\*Corresponding author: choi@atr.jp

necessary for the achievement of single-mode lasing. The lasing threshold current is measured as 81 mA. The laser shows stable single-mode lasing for the pumping current below 132 mA. We show the spectrum data for single-mode lasing at the pumping current 90 mA in Fig. 1(a). The achievement of the single-mode lasing is assured by two experimental evidence. One is that the FWHM of the peak in Fig. 1(a) is 0.017 nm, which is less than the wave numerical estimate of the average mode spacing 0.055 nm. This estimate is based on the systematic analysis of cavity modes found for the frequency range  $60.94 \leq \text{Re } kR \leq 61.02$  (i.e.,  $1545 \text{ nm} \leq \lambda \leq 1547 \text{ nm}$ ), where 34 modes are detected. When solving the equations, we assume transverse-electric(TE) polarization, taking into account that the measured light is TE-polarized. The cavity modes are solutions of the Maxwell equations for a stadium-shaped cavity without gain [13]. The other evidence is that, below 132 mA, the far-field emission pattern does not change for the increase of the pumping current, except for overall linear intensity growth. At the pumping current 132 mA, another lasing mode emerges and the number of lasing modes grows continuously as the pumping current increases. For instance, at 270 mA, we observed 8 lasing modes in the spectrum as shown in Fig. 1(b).

### 3 Far-field characteristics of single- and multi-mode lasing

Figures 2(a) and 2(b) show the far-field patterns for single-mode lasing at 100 mA and for multi-mode lasing at 270 mA, respectively. We note that the intensity is normalized in both far-field patterns so that the intensity integration over all angles becomes unity. Moreover, spatial oscillations smaller than 0.8 degrees are smeared out because of the resolution limit of our measurement. In Figs. 2(a) and 2(b), we also plotted the result of a ray simulation. The ray simulation is based on the dynamics of an ensemble of rays inside the cavity taking into account the ray emission at the cavity boundary described by Fresnel's law. The method of the ray simulation is explained in detail in Refs. [6, 7]. Comparing Figs. 2(a) and 2(b), we find that the oscillation amplitude of the far-field pattern is larger in the single-mode lasing case than in the multi-mode lasing case. Moreover, in the multi-mode lasing case, the variation trend of the far-field pattern can be well explained by the ray simulation result.

For better understanding of these experimental results, we performed wave numerical calculation of far-field patterns. We investigated 74 cavity modes with high quality factors sampled from the frequency range,  $60.00 \leq \text{Re } kR \leq 61.40$  (i.e.,  $1535 \text{ nm} \leq \lambda \leq 1571 \text{ nm}$ ) and  $-0.04 \leq \text{Im } kR \leq 0.0$ . We emphasize that this frequency range corresponds to the range relevant for our experiments. Figure 2(c) is the far-field pattern of a high quality factor mode whose frequency,  $\text{Re } kR = 60.96536$  (i.e.,  $\lambda = 1545.9 \text{ nm}$ ) and  $\text{Im } kR = -0.02385$ , is close to the single-mode lasing frequency,  $\lambda = 1545.7 \text{ nm}$ . We see that the large-amplitude oscillation observed in the single-mode lasing experiment is well reproduced in Fig. 2(c), although we cannot make an exact correspondence of peak positions between Fig. 2(a) and 2(c). We note that the large-amplitude oscillation of a far-field pattern is not a peculiar feature of the cavity mode shown in Fig. 2(c) but a common feature of all the cavity modes. The far-field pattern of the multi-mode lasing can be approximated by the average of the far-field patterns of multiple cavity modes. The pattern obtained by averaging 8 cavity modes is shown in Fig. 2(d), where one can observe that, as in the multi-mode lasing experiment, the oscillation amplitude becomes smaller and the variation trend exhibits better agreement with the ray simulation result compared to the single-mode case.

The correspondence of wave numerical results with the ray simulation result can be confirmed more clearly for a larger cavity. In Fig. 2(e), we plot wave numerical results for a stadium-shaped cavity with  $R = 30 \mu\text{m}$ , which is twice as large as the one in our experiments. We plot in Fig. 2(e) the averaged far-field pattern for 8 cavity modes (green curve) and that for 54 cavity modes (black curve) together with the ray simulation result (red broken curve), where one can clearly observe the convergence of the wave numerical results onto the ray simulation result by increasing the number of averaged modes.

### 4 Spectral decomposition of a multi-mode lasing state

The experimental far-field patterns shown in Fig. 2(a) and 2(b) are measured by a photodetector. Using a monochromator instead, we can measure the far-field patterns for individual lasing modes for the multi-mode lasing state for the pumping current 270 mA. In Fig. 3, we plot the far-field patterns corresponding to 6 dominant lasing modes in Fig. 1(b), measured by a monochromator(Ando AQ6317C) whose transmission band width is 0.01 nm. We note that rapid spatial oscillations smaller than 0.24 degrees are smeared out in the measurement. As expected from the analysis of the cavity modes in the

previous section, each of the lasing modes is found to have a less similar pattern with the result of a ray simulation. We note that mode C in Fig. 3 is nothing but the mode shown in Fig. 2(a). The agreement of the far-field pattern of mode C and that of the single-mode lasing at 100 mA convinces us the consistency between the measurements by the photodetector and by the monochromator. The existence of a variety of patterns in lasing modes as shown in Fig. 3 is contrasted with the previous work on the quadrupole-deformed cavity [14], where all lasing modes are found to have far-field patterns closely corresponding to a ray simulation result. On the basis of our present result and previous theoretical analysis [7], we conclude that in general (i.e., for a generic cavity shape with an arbitrary refractive index) the good correspondence with a ray simulation result can not always be observed for the far-field pattern of a single lasing mode, but can be observed for the averaged far-field pattern such as those realized in multi-mode lasing.

## 5 Discussion

In the experimental and wave numerical far-field patterns, one finds that the spatial oscillations around the 90 degrees are more rapid than those in the other range. This can be explained in the following manner: From numerical analysis of cavity modes together with the analysis of a ray model, we find that light is mostly emitted from the two semi-circular parts of the stadium. Thus, one can suppose that far-field emission pattern around 90 degrees is the interference pattern of the light coming from the two semi-circular parts. Since the two light sources (i.e., two semi-circular parts) are located very close, they result in rapid oscillation in the far-field emission pattern. Approximating the distance of the two light sources as  $3R = 45 \mu\text{m}$ , one can estimate the period of the interference pattern as 2 degrees, which is consistent with both the experimental data in Fig. 3 and the numerical data in Fig. 2(c). On the other hand, the far-field pattern around, say, 0 degree is supposed to be composed of light coming from one light source (i.e., one semi-circular part). Thus, for this angle range, one finds no rapid oscillation due to the interference.

Lastly, we remark on the asymmetry of the far-field patterns observed in Figs. 2(a) and 3. In theory, the far-field patterns of individual cavity modes obey the  $C_{2v}$  symmetry of the stadium shape. However, some of the measured patterns in Figs. 2(a) and 3 (e.g. mode F) exhibit noticeable asymmetries. It is difficult to attribute these asymmetries to extrinsic imperfections involved in the fabrication and measurement, since we have also observed a rather symmetric pattern (e.g. mode A) for the same cavity. A plausible explanation is that an asymmetric lasing mode corresponds not to a single cavity mode but multiple cavity modes with their frequencies locked to a single frequency. It has been demonstrated experimentally and numerically that multiple frequency-locked modes can generate asymmetric emission patterns [5].

## 6 Conclusion

We studied spectral and far-field characteristics of stadium-shaped InGaAsP microlasers. We experimentally achieved single-mode lasing and showed that the observed large-amplitude oscillations in the far-field pattern can be reproduced by wave numerical calculation of cavity modes. For the far-field pattern for multi-mode lasing, we found the oscillation amplitude is suppressed and the global variation trend can be well explained by a ray simulation result, which is also reproduced by the wave numerical calculation. These results are evidence for a hypothesis [7] that the correspondence with a ray simulation becomes better as a result of multi-mode lasing.

## Acknowledgments

The authors greatly thank Prof. Takehiro Fukushima for helpful suggestions. The work at ATR was supported in part by the National Institute of Information and Communications Technology of Japan.

## References

- [1] K. J. Vahala, "Optical microcavities," *Nature* **424**, 839-846 (2003).

- [2] J. U. Nöckel and A. D. Stone, “Ray and wave chaos in asymmetric resonant optical cavities,” *Nature* **385**, 45-47 (1997).
- [3] For example, H. G. L. Schwefel, H. E. Türeci, A. D. Stone and R. K. Chang, “Progress in Asymmetric Resonant Cavities: Using Shape as a Design Parameter in Dielectric Microcavity Lasers,” in *Optical Processes in Microcavities*, K. Vahala ed. (World Scientific, Singapore, 2005), pp. 415-496.
- [4] L. A. Bunimovich, “On the ergodic properties of nowhere dispersing billiards,” *Commun. Math. Phys.* **65**, 295-312 (1977).
- [5] T. Harayama, S. Sunada and K. S. Ikeda, “Theory of two-dimensional microcavity lasers,” *Phys. Rev. A* **72**, 013803 (2005).
- [6] S. Shinohara, T. Harayama, H. E. Türeci, and A. D. Stone, “Ray-wave correspondence in the non-linear description of stadium-cavity lasers,” *Phys. Rev. A* **74**, 033820 (2006); S. Shinohara and T. Harayama, “Signature of ray chaos in quasibound wave functions for a stadium-shaped dielectric cavity,” *Phys. Rev. E* **75**, 036216 (2007).
- [7] S. Shinohara, T. Fukushima and T. Harayama, “Light emission patterns from stadium-shaped semiconductor microcavity lasers,” *Phys. Rev. A* **77**, 033807 (2008).
- [8] T. Fukushima and T. Harayama, “Stadium and quasi-stadium laser diodes,” *IEEE Sel. Top. Quantum Electron.* **10**, 1039-1051 (2004).
- [9] W. Fang, H. Cao, and G. S. Solomon, “Control of lasing in fully chaotic open microcavities by tailoring the shape factor,” *Appl. Phys. Lett.* **90**, 081108 (2007).
- [10] H. -G. Park, F. Qian, C. J. Barrelet and Y. Li, “Microstadium single-nanowire laser,” *Appl. Phys. Lett.* **91**, 251115 (2007).
- [11] M. Lebental, J. S. Lauret, R. Hierle, and J. Zyss, “Highly directional stadium-shaped polymer micro-lasers,” *Appl. Phys. Lett.* **88**, 031108 (2006); M. Lebental, J. S. Lauret, J. Zyss, C. Schmit, and E. Bogomolny, “Directional emission of stadium-shaped microlasers,” *Phys. Rev. A* **75**, 033806 (2007).
- [12] T. Fukushima, T. Tanaka and T. Harayama, “Ring and axis mode switching in multielectrode strained InGaAsP multiple-quantum-well quasistadium laser diodes,” *Appl. Phys. Lett.*, **87**, 191103 (2005).
- [13] J. Wiersig, “Boundary element method for resonances in dielectric microcavities,” *J. Opt. A: Pure Appl. Opt.* **5**, 53-60 (2003).
- [14] J.-B. Shim, S.-B. Lee, J. Yang, S. Moon, J.-H. Lee, K. An, H.-W. Lee, and S. W. Kim, “Regular Spectra and Universal Directionality of Emitted Radiation from a Quadrupolar Deformed Microcavity,” *J. Phys. Soc. Jpn.* **76**, 114005 (2007).

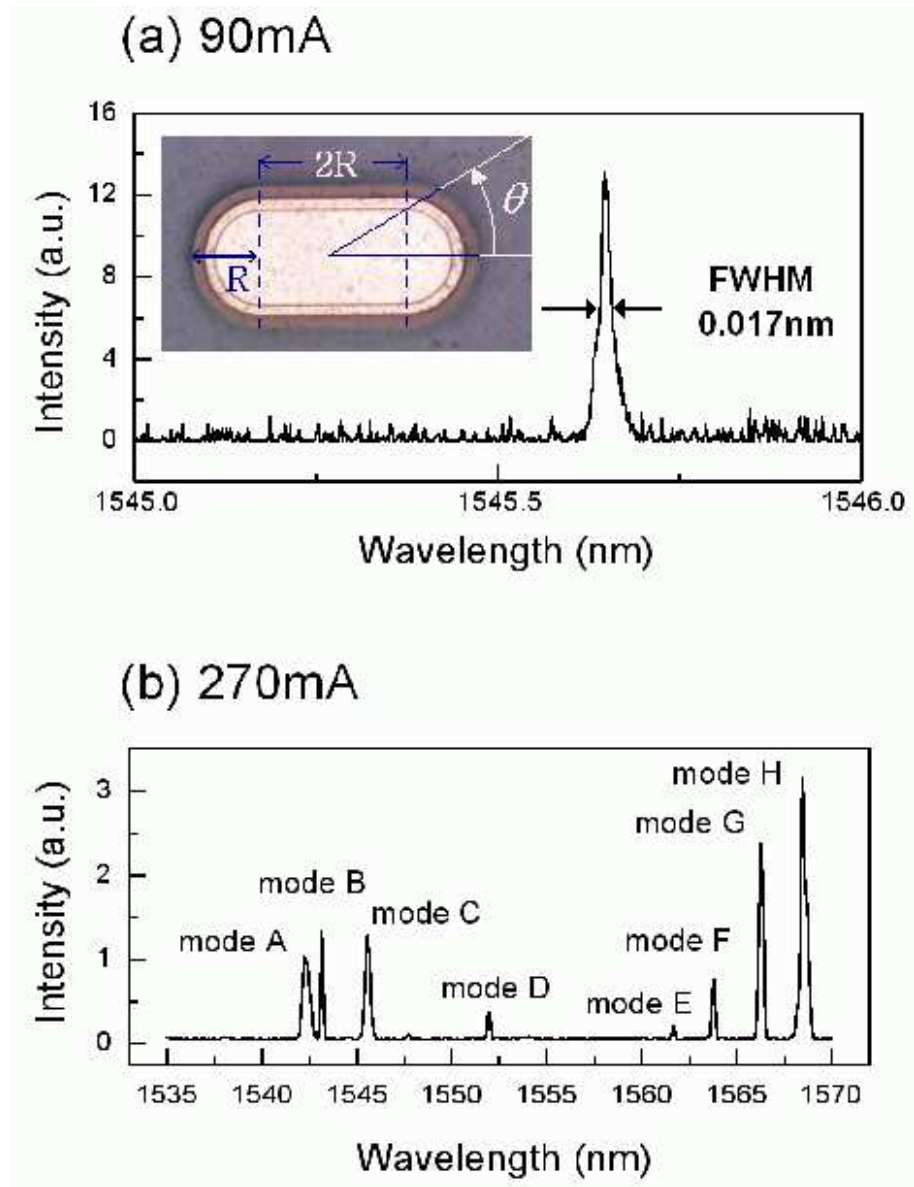


Figure 1: Lasing spectra for the stadium-shaped InGaAsP microlaser. (a) Single-mode lasing at pumping current 90 mA. The inset shows the microscope image of the Bunimovich stadium. (b) Multi-mode lasing at 270 mA.

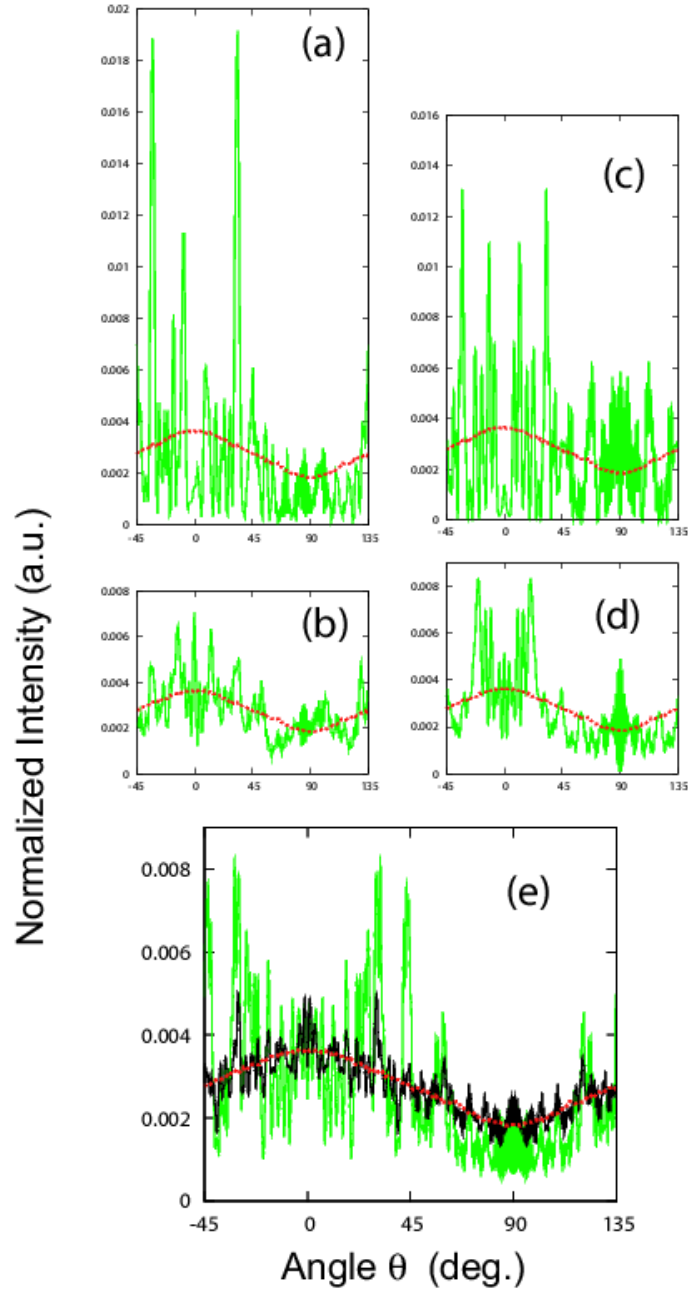


Figure 2: Far-field patterns for experiments (green curves in (a) and (b)) and for wave numerical simulations (green and black curves in (c), (d) and (e)). In (a)-(e), ray simulation data are plotted by a red broken curve. (a) Experimental single-mode lasing data for the pumping current 100 mA. (b) Experimental multi-mode lasing data for 270 mA. (c) Wave calculation data of a single cavity mode. (d) Wave calculation data of the average of 8 cavity modes. These wave calculations are performed for a cavity with  $R = 15 \mu\text{m}$ , which is the cavity size of our experiments. (e) Wave calculation data for a cavity with  $R = 30 \mu\text{m}$ , where the averaged far-field pattern for 8 cavity modes is plotted by a green curve, while that for 54 cavity modes is plotted by a black curve.

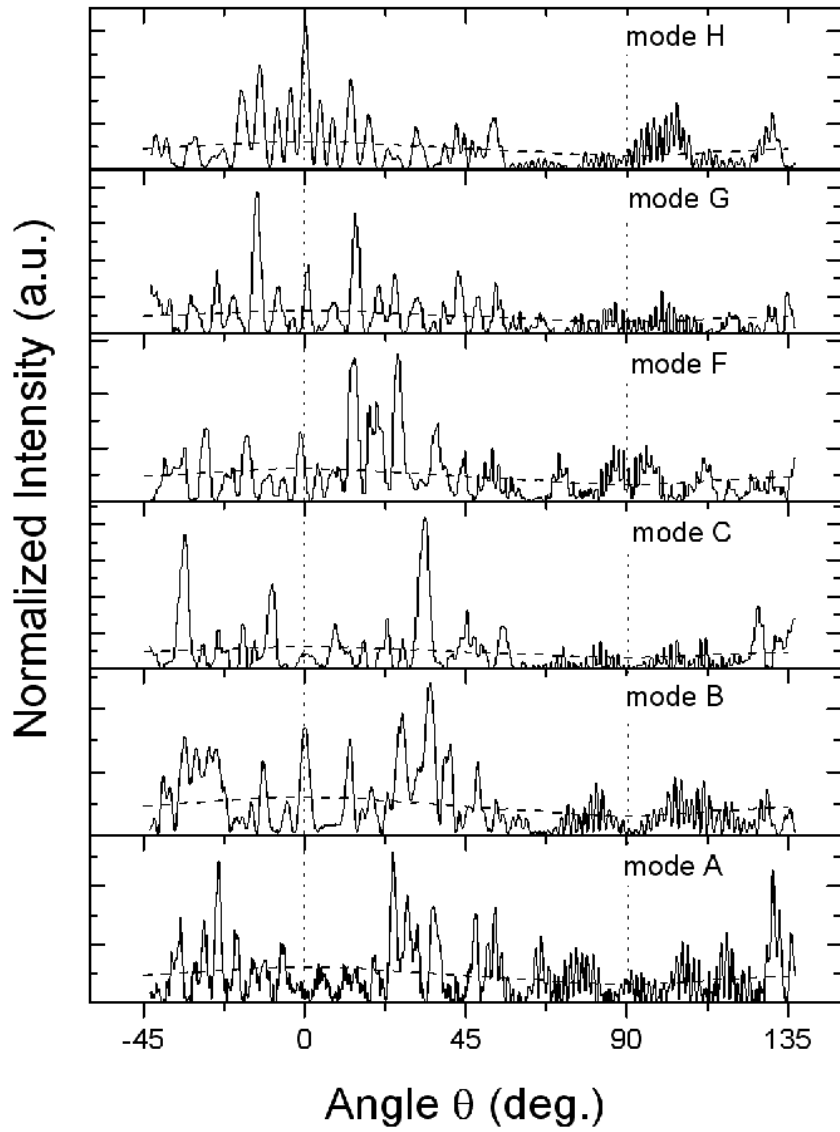


Figure 3: Far-field patterns for the 6 dominant lasing modes for the pumping current 270 mA. The data are measured by a monochromator. The labeling of the lasing modes corresponds to that in Fig. 1(b). The result of a ray simulation is plotted in dashed curves.